

Tachyon Kinks in Boundary String Field Theory

Chanju Kim

Department of Physics, Ewha Womans University, Seoul 120-750, Korea

`cjkim@ewha.ac.kr`

Yoonbai Kim and O-Kab Kwon

BK21 Physics Research Division and Institute of Basic Science,

Sungkyunkwan University, Suwon 440-746, Korea

`yunbai@skku.edu` `okab@skku.edu`

Ho-Ung Yee

Korea Institute for Advanced Study,

207-43 Cheongryangri 2-dong Dongdaemun-gu, Seoul 130-722, Korea

`ho-ung.yee@kias.re.kr`

Abstract

We study tachyon kinks with and without electromagnetic fields in the context of boundary string field theory. For the case of pure tachyon only an array of kink-antikink is obtained. In the presence of electromagnetic coupling, all possible static codimension-one soliton solutions such as array of kink-antikink, single topological BPS kink, bounce, half kink, as well as nonBPS topological kink are found, and their properties including the interpretation as branes are analyzed in detail. Spectrum of the obtained kinks coincides with that of Dirac-Born-Infeld type effective theory.

1 Introduction

Study on the unstable systems of D-branes has been an attractive subject in string theory; for example, an unstable D-brane or $D\bar{D}$ [1]. An intriguing issue among various questions is the pattern of remnant after the unstable Dp -brane or $Dp\bar{D}p$ decays completely. Since perturbative open string degrees of freedom should disappear in the absence of the original branes, the remained fossils can be either closed strings or nonperturbative objects in open string theory.

When nonperturbative open string degrees of freedom are considered in a form of solitonic objects, a lesson from quantum field theories dealing with spontaneous symmetry breaking is that we should employ a scheme of semi-classical approximation. There are several appropriate languages describing open string tachyons and the solitonic lower dimensional branes, including boundary conformal field theory (BCFT) [2, 3], boundary string field theory (BSFT or background-independent string field theory) [4, 5, 6, 7], effective field theory (EFT) [8, 9, 10], and noncommutative field theory (NCFT) in the presence of fundamental strings [11]. If we want to take into account string off-shell contributions, BSFT fits its purpose. However, most of the previous studies have been made in the context of Dirac-Born-Infeld (DBI) type tachyon EFT with runaway potential, avoiding the complicated kinetic term of the BSFT action [4, 5, 12].

In BSFT, decent relations for the codimension-one and -two branes were obtained in exact form from the energy density difference between the false and true vacua [4, 5], but the corresponding smooth solitonic solutions of the equations of motion have not been analyzed before in BSFT. On the other hand, the tachyon kinks [9, 7, 10, 13, 14], tubes [15], and vortices [9, 16] have been found by examining the equations of motion from the DBI type EFT. Specifically, for the case of tachyon kinks, pure tachyon can support only an array of kink-antikink [7, 10]. In the presence of the DBI electromagnetic fields, the spectrum of the kinks solutions becomes richer; they include array of kink-antikink, single topological BPS kink, bounce, half-kink, as well as topological nonBPS kink [10, 17]. Moreover, with the $1/\cosh$ -type tachyon potential, analytic solutions are available [10] and their tachyon profiles can be mapped to those in BCFT by Ref. [18]. These kink solutions are also reproduced in NCFT [19].

In this paper, we study the effective action from BSFT with worldsheet supersymmetry and find all the aforementioned tachyon kinks as solutions of classical equations of motion. Moreover, the solution of single topological BPS kink with critical DBI electromagnetic field is given in a closed form, so that the exact solution may be useful in studying the relation between BCFT and BSFT. The species of the tachyon kinks coincide with those

in the DBI type EFT, but they show slight difference in some minor details such as shape of energy density. This seems to suggest a need of further study in BCFT. Since only array of kink-antikink and single topological BPS kink were discovered in BCFT with electromagnetic coupling [3], it would be intriguing if we reproduce other three kinks (bounce, half kink, topological nonBPS kink) in the context of BCFT [20]. The former two kink configurations can easily be interpreted as array of $D(p-1)\bar{D}(p-1)$ or $D(p-1)F1\bar{D}(p-1)F1$ and single thick $D(p-1)$ or $D(p-1)F1$. Though we discuss some interpretations as brane configurations, the other three kink configurations await proper understanding in string theory.

In section 2 we briefly review a derivation of the super BSFT action with a real tachyon and DBI type electromagnetic field, and derive its classical equations of motion. In sections 3 and 4, we consider the tachyon without and with DBI type electromagnetic field respectively, and find all possible static kink solutions from the equations of motion. The obtained spectrum of the kinks coincides with that from DBI type EFT and NCFT. Section 5 contains our conclusions with brief outlook for further study. Appendix A includes detailed calculations of array of kink-antikink, and appendix B deals with comparison of the tachyon kinks between super and bosonic BSFTs.

2 BSFT Setup

In this section we briefly recapitulate derivation of the BSFT action of the real tachyon and gauge field on an unstable Dp -brane in superstring theory. According to the BV-like formulation of BSFT for open string [21], the off-shell BSFT action is identical to the disc partition function [22] including gauge fields [23] and tachyon [5, 12];

$$S = Z. \quad (2.1)$$

For an unstable Dp -brane, the partition function is given by

$$Z = \int [\mathcal{D}X^\mu][\mathcal{D}\psi^\mu][\mathcal{D}\bar{\psi}^\mu] \exp[-(S_{\text{bulk}} + S_{\text{bdry}})], \quad (2.2)$$

where the bulk action S_{bulk} and the boundary action S_{bdry} are

$$S_{\text{bulk}} = \frac{1}{4\pi} \int_{\Sigma} d^2z \left(\partial X^\mu \bar{\partial} X_\mu + \psi^\mu \bar{\partial} \psi_\mu + \bar{\psi}^\mu \partial \bar{\psi}_\mu \right), \quad (2.3)$$

$$S_{\text{bdry}} = \int_{\partial\Sigma} \frac{d\tau}{2\pi} \left[\frac{1}{4} T^2 - \frac{1}{2} \psi^\mu \partial_\mu T \partial_\tau^{-1} (\psi^\nu \partial_\nu T) + \frac{i}{2} F_{\mu\nu} \psi^\mu \psi^\nu - \frac{i}{2} A_\mu \frac{dX^\mu}{d\tau} \right]. \quad (2.4)$$

Here Σ denotes a disc with unit radius in the Euclidean worldsheet with complex coordinates (z, \bar{z}) , and its boundary is $\partial\Sigma$ with coordinate τ ($0 \leq \tau \leq 2\pi$). Note that we set $\alpha' = 2$ and contributions from ghost sector are decoupled.

Let us consider a relevant linear profile of the tachyon

$$T(X) = u_\mu X^\mu, \quad (2.5)$$

and a constant electromagnetic field strength $F_{\mu\nu}$ with symmetric gauge $A_\mu = -F_{\mu\nu}X^\nu/2$. Performing functional integration of the worldsheet fields, we obtain an action in a closed form

$$S = Z = Z_F Z_B \quad (2.6)$$

$$\sim \int d^d x e^{-\frac{1}{4}T^2} \frac{\prod_{r=\frac{1}{2}}^\infty \det(\eta_{\mu\nu} + \frac{1}{r}\partial_\mu T \partial_\nu T + F_{\mu\nu})}{\prod_{n=1}^\infty \det(n\eta_{\mu\nu} + \partial_\mu T \partial_\nu T + nF_{\mu\nu})}, \quad (2.7)$$

where Z_F and Z_B are fermionic and bosonic parts of the worldsheet partition function, respectively. The action (2.7) is written as a divergent infinite product, and through zeta function regularization, we obtain a well-defined finite action of the tachyon and the DBI electromagnetic field. The result is

$$S(T, A_\mu) = -\mathcal{T}_p \int d^d x V(T) \sqrt{-\det(\eta_{\mu\nu} + F_{\mu\nu})} \mathcal{F}(y), \quad (2.8)$$

where the potential is

$$V(T) = e^{-\frac{1}{4}T^2}, \quad (2.9)$$

and the kinetic piece is

$$\mathcal{F}(y) = \frac{4^y y \Gamma(y)^2}{2\Gamma(2y)} = 2^{2y-1} y B(y, y) = y \int_{-1}^1 dx (1-x^2)^{y-1} \quad (2.10)$$

with $y = \left(\frac{1}{\eta+F}\right)^{\mu\nu} \partial_\mu T \partial_\nu T$. We also fix the overall normalization by the tension \mathcal{T}_p of the unstable Dp-brane.

It is straightforward to derive the equations of motion. For tachyon field, it reads as

$$\partial_\mu \left[V \sqrt{-\det(\eta + F)} \frac{d\mathcal{F}}{dy} \left(\frac{1}{\eta + F} \right)_S^{\mu\nu} \partial_\nu T \right] = \frac{1}{2} \sqrt{-\det(\eta + F)} \mathcal{F} \frac{dV}{dT}, \quad (2.11)$$

while for gauge field, it can be written as

$$\partial_\mu \Pi^{\mu\nu} = 0 \quad (2.12)$$

with the antisymmetric displacement tensor $\Pi^{\mu\nu}$ given by

$$\begin{aligned} \Pi^{\mu\nu} \equiv \frac{\delta S}{\delta \partial_\mu A_\nu} = & \mathcal{T}_p V \sqrt{-\det(\eta + F)} \left[\left(\frac{1}{\eta + F} \right)_A^{\mu\nu} \mathcal{F} + \right. \\ & \left. 2 \left(\left(\frac{1}{\eta + F} \right)_A^{\rho\mu} \left(\frac{1}{\eta + F} \right)_S^{\sigma\nu} - \left(\frac{1}{\eta + F} \right)_A^{\rho\nu} \left(\frac{1}{\eta + F} \right)_S^{\sigma\mu} \right) \frac{d\mathcal{F}}{dy} \partial_\rho T \partial_\sigma T \right]. \end{aligned} \quad (2.13)$$

For the tachyon equation (2.11), it is possible to consider conservation of energy-momentum instead,

$$\partial_\mu T^{\mu\nu} = 0, \quad (2.14)$$

where the energy-momentum tensor read from the above action is

$$\begin{aligned} T^{\mu\nu} = & -\mathcal{T}_p V(T) \sqrt{-\det(\eta + F)} \left\{ \mathcal{F}(y) \left(\frac{1}{\eta + F} \right)_S^{\mu\nu} \right. \\ & \left. - \frac{d\mathcal{F}}{dy} \left[\left(\frac{1}{\eta + F} \right)^{\alpha\mu} \left(\frac{1}{\eta + F} \right)^{\nu\beta} + \left(\frac{1}{\eta + F} \right)^{\alpha\nu} \left(\frac{1}{\eta + F} \right)^{\mu\beta} \right] \partial_\alpha T \partial_\beta T \right\}. \end{aligned} \quad (2.15)$$

We are interested in static kink configurations satisfying the above equations of motion (2.11)–(2.12), and we will interpret the obtained solitons as codimension one, BPS composites of $D(p-1)$ -branes and fundamental strings. The case of pure tachyon field with vanishing electromagnetic field is considered in section 3, and we analyze the case with electromagnetic field turned on in section 4.

3 Array of $D(p-1)\bar{D}(p-1)$ as Tachyon Kink

We begin this section with turning off the gauge field $F_{\mu\nu} = 0$ and considering a simple case of the pure tachyon field. Then the equation of the gauge field (2.12) is trivially satisfied. To construct flat codimension-one soliton configurations by examining the classical tachyon equation (2.11), we naturally introduce an ansatz

$$T = T(x), \quad (3.1)$$

where x is one of spatial coordinates.

For the case of pure tachyon, substitution of the ansatz (3.1) makes the equations (2.14) simple, i.e., the only equation we have to solve is that the parallel component of the pressure should be constant; $\frac{dT^{11}}{dx} \equiv (T^{11})' = 0$, where

$$T^{11} = -\mathcal{T}_p V(T) G(y) = -\mathcal{T}_p e^{-\frac{1}{4}T^2} G(y), \quad y = T'^2 \geq 0, \quad (3.2)$$

and the function $G(y)$ defined by

$$G(y) = \mathcal{F}(y) - 2y\dot{\mathcal{F}}(y), \quad \dot{\mathcal{F}}(y) = \frac{d\mathcal{F}}{dy}, \quad (3.3)$$

is monotonically-decreasing from $G(0) = 1$ to $G(\infty) = 0$. Introducing functions

$$K(y) = \frac{1}{G(y)^2} - 1, \quad (3.4)$$

$$U(T) = -\left(\frac{\mathcal{T}_p V(T)}{T^{11}}\right)^2 = -\left(\frac{\mathcal{T}_p}{T^{11}}\right)^2 e^{-\frac{1}{2}T^2}, \quad (3.5)$$

we rewrite the equation (3.2) as

$$\mathcal{E} = K(T'^2) + U(T). \quad (3.6)$$

where $\mathcal{E} = -1$, $K(y)$ is a positive, monotonically-increasing function with the minimum $\min(K) = 0$ at $y = 0$, and the profile of $U(T)$ has $\min(U) = U(0) = -(\mathcal{T}_p/T^{11})^2$ and is monotonically-increasing to $\max(U) = U(T = \pm\infty) = 0$. Suppose we consider one-dimensional motion of a hypothetical particle at a position T and time x with conserved mechanical energy \mathcal{E} and velocity T' . Then the position-dependent function $U(T)$ may be identified as a kind of “potential” and the velocity-dependent function $K(T'^2)$ as a kind of “kinetic energy”. The reason for choosing this form of kinetic term $K(T'^2)$ (3.4) is that it becomes quadratic in T' both in $|T'| \rightarrow 0$ and $|T'| \rightarrow \infty$ limits:

$$K(T'^2) \rightarrow \begin{cases} \frac{16}{\pi} T'^2 + (-1 - \frac{4}{\pi}) + \mathcal{O}(|T'|^{-2}), & |T'| \rightarrow \infty \\ (4 \log 2) T'^2 + \mathcal{O}(|T'|^4), & |T'| \rightarrow 0 \end{cases} \quad (3.7)$$

so that it mimics a right kind of kinetic term. Fig. 1 shows the graphs of $K(T'^2)$ and $U(T)$.

From this, we see that there always exists a nontrivial *oscillating* solution $T(x)$ when $U(0) = -(\mathcal{T}_p/T^{11})^2 < -1$. At the maximum of $|T(x)|$, we have $T' = 0$ and (3.6) gives the maximum value,

$$T_{\max} = 2\sqrt{\ln |\mathcal{T}_p/T^{11}|}. \quad (3.8)$$

Since no exact solution is obtained in closed form, we plot numerical solutions in Fig. 2. This solution can be interpreted as an array of kink-antikink pairs.

We also find from the ansatz (3.1) that the momentum density vanishes, $T^{01} = 0$, and the energy density is the only quantity involving local physical character

$$T^{00} = \mathcal{T}_p V(T) \mathcal{F}(T'^2) = \mathcal{T}_p e^{-\frac{1}{4}T^2} \mathcal{F}(T'^2). \quad (3.9)$$

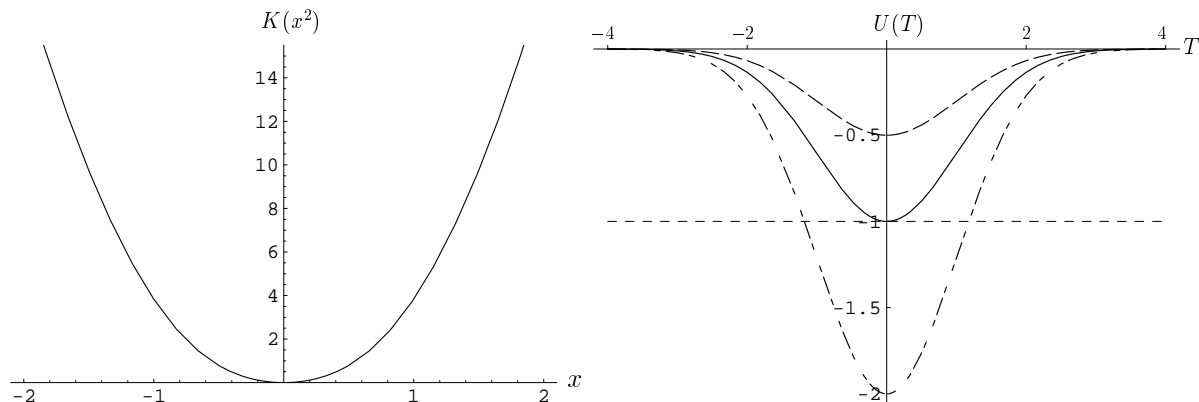


Figure 1: The graphs of $K(T'^2)$ (left) and $U(T)$ (right). For $U(T)$, three cases of $\mathcal{T}_p/(-T^{11}) = 1/\sqrt{2}$ (dashed curve), 1 (solid curve), $\sqrt{2}$ (dotted-dashed curve) from top to bottom are shown. $\mathcal{E} = 1$ is denoted by dotted line.

For the obtained solution, the energy density of a single kink (antikink) is shown in Fig. 3 for several T_{\max} . We see that the energy is obviously accumulated at the site of kink (antikink).

Note that, in Fig. 2, a kink and its adjacent antikink gets closer as T_{\max} becomes larger (or, equivalently, $-T^{11}$ becomes smaller). This is in contrast with the array solution in DBI-type EFT with $1/\cosh$ potential where the distance is constant regardless of the value of T^{11} [10]. Therefore it is interesting to find how the distance changes as we vary the negative pressure $-T^{11}$ which is the only parameter governing the array solution.

Let us first consider the limit $-T^{11} \rightarrow \mathcal{T}_p$ which corresponds to $T_{\max} \rightarrow 0$, i.e., the solution represents a small fluctuation around vacuum. Then we have a harmonic oscillator solution

$$T(x) \approx T_{\max} \sin\left(\frac{2\pi}{\xi_0} x\right), \quad (3.10)$$

where the width ξ_0 is equal to $2\pi\sqrt{2\log 2} \approx 7.39$.

In the opposite limit of $T_{\max} \rightarrow \infty$ or $T^{11} \rightarrow 0$, complicated nature of the “kinetic” term $K(T'^2)$ comes into play and a careful investigation is needed. Since the analysis is rather technical, here we will only sketch the argument. Details can be found in Appendix A. First observe from Fig. 2 that the array solution can be divided roughly into three regions, namely the region around (anti)kink sites where the slope of the tachyon profile is steep, plateau region where there is almost no change in $T(x)$, and the transition region which connects the other two regions. From the figure it is easy to guess that the width of the (anti)kink region goes to zero in $T^{11} \rightarrow 0$ limit. Then it remains to estimate the

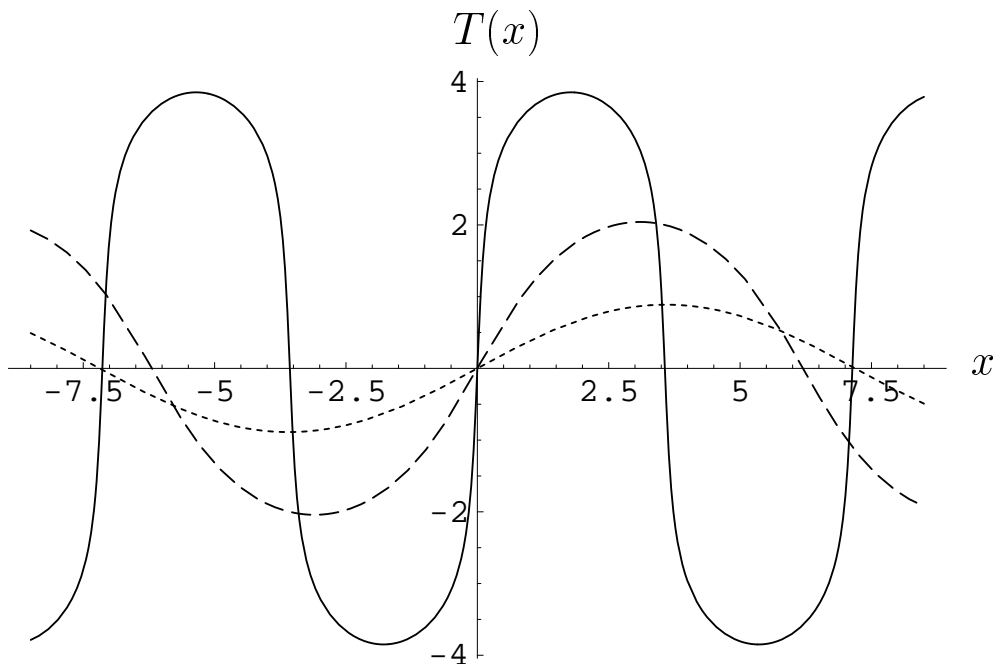


Figure 2: Profiles of array of kink-antikink for the cases $T_{\max} = 1, 2, 3.8$ from bottom to top are shown. It is clear that their width is decreasing as T_{\max} increases.

distance of the other two regions. According to the analysis of Appendix A, the result is that actually the width of the other regions also vanishes as T^{11} goes to zero. This behavior is essentially related with large T behavior of the potential which vanishes faster than e^{-T} in this theory. This is in accordance with the results in DBI type EFT [13, 14].

Finally, we come to the question of energy density in large T_{\max} limit. As seen in Fig. 3, the energy stored in the plateau region and the transition region is negligible. (This is shown more rigorously in Appendix A.) Since T'^2 becomes very large in (anti)kink region, we can approximate $\mathcal{F}(T'^2) \approx \sqrt{\pi} T'$ and the energy integral for a kink becomes

$$\int T^{00} dx \approx \sqrt{\pi} \mathcal{T}_p \int e^{-\frac{1}{4}T^2} T' dx = \sqrt{\pi} \mathcal{T}_p \int e^{-\frac{1}{4}T^2} dT. \quad (3.11)$$

This becomes exact as $T_{\max} \rightarrow \infty$ ($T^{11} \rightarrow 0$) and hence

$$\mathcal{T}_{p-1} = \sqrt{\pi} \mathcal{T}_p \int_{-\infty}^{\infty} e^{-\frac{1}{4}T^2} dT = 2\pi \mathcal{T}_p = (2\pi\sqrt{\alpha'}) \frac{\mathcal{T}_p}{\sqrt{2}}, \quad (3.12)$$

reproducing the tension of BPS $D(p-1)$ brane.

To summarize, pressureless limit leads to the BPS kink which interpolates two tachyon vacua $T = \pm T_{\max} = \pm\infty$ with right tension and the obtained static regular configuration

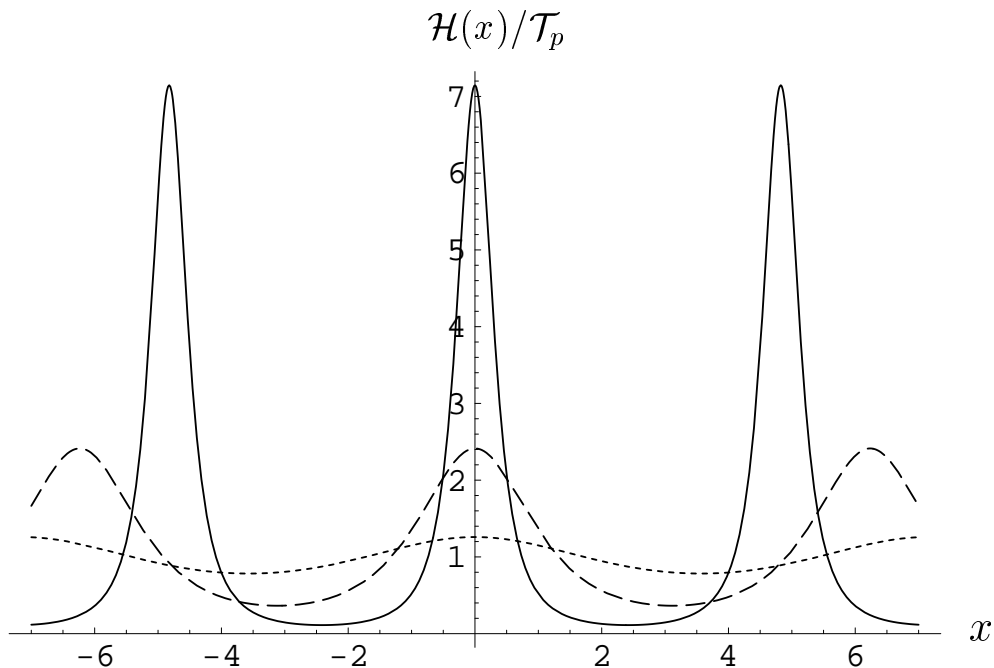


Figure 3: Energy density profiles of single kink (antikink) for the cases $T_{\max} = 1, 2, 3$ from bottom to top are shown. It is clear that their width is decreasing as T_{\max} increases.

describes an array of kink-antikink, which is the same as the soliton spectrum in DBI type EFT and BCFT. In the context of superstring theory, it is interpreted as an array of $D(p-1)\bar{D}(p-1)$.

4 Codimension-one Branes from Tachyon and Electromagnetic Field

If we turn on DBI electromagnetic field $F_{\mu\nu}$ on the unstable Dp -brane, the analyses based on DBI type EFT [10, 17], BCFT [3], and NCFT [19] showed that spectrum of the regular kinks and their composites becomes rich. To be specific, the ansatz for codimension-one objects,

$$F_{\mu\nu} = F_{\mu\nu}(x), \quad (4.1)$$

was made for DBI electromagnetic field in EFT and NCFT, but the classical equations dictate it to be constant which is consistent with the assumption in BCFT. Examining the remained equations, they obtained various kinds of static kink configurations. For $p = 1$, array of kink-antikink, single topological BPS kink, and topological non-BPS kink

have been found in both EFT and NCFT but only first two of them were identified in BCFT. For $p \geq 2$, in EFT and NCFT, three more types of kinks were found in addition to the above three, i.e., they are bounce, half kink, and hybrid of two half kinks (we call the hybrid as another topological nonBPS kink in what follows), however they have not been identified in BCFT. Furthermore, proper interpretation of the kink configurations which are not found in the context of BCFT has not been made, yet.

Since BSFT is valid for description of off-shell physics of the string theory and its classical limit arrives at a BCFT, it is an appropriate scheme to reconcile this discrepancy. In the following two subsections, we investigate static kink solutions in BSFT and interpret the obtained solutions in terms of D-branes and their composites with fundamental strings.

4.1 $p = 1$

When we have an unstable D1-brane, there exist a tachyon field and an electric field component $E = -F_{01}$. For static objects, the equations we have to deal with reduce to the conservation of energy-momentum (2.14), $(T^{11})' = 0$,

$$T^{11} = -\frac{\mathcal{T}_1 V}{\sqrt{1-E^2}} \left(\mathcal{F} - \frac{2T'^2}{1-E^2} \dot{\mathcal{F}} \right) = \text{constant}, \quad (4.2)$$

and the gauge equation (2.12), $(\Pi)' = 0$,

$$\Pi \equiv \frac{\delta S}{\delta(\partial_0 A^1)} = -\frac{\mathcal{T}_1 V E}{\sqrt{1-E^2}} \left(\mathcal{F} - \frac{2T'^2}{1-E^2} \dot{\mathcal{F}} \right) = \text{constant}. \quad (4.3)$$

Since the constant pressure T^{11} (4.2) and the constant fundamental string charge density Π (4.3) lead to constant electric field $E = \Pi/T^{11}$, we have a single nontrivial equation, (4.2) or (4.3), and the obtained solutions can be classified by two constant parameters Π and E .

In the following, it is convenient to introduce a rescaled spatial coordinate

$$\tilde{x} = \sqrt{1-E^2} x. \quad (4.4)$$

Then, with the static ansatz (3.1), the variable y defined in (2.10) becomes

$$y = \frac{T'^2}{1-E^2} \equiv \tilde{T}'^2. \quad (4.5)$$

With the rescaled coordinate \tilde{x} , the action with constant electric field takes the form

$$\begin{aligned} \frac{S}{-\int dt} &= \mathcal{T}_1 \int dx e^{-\frac{T^2}{4}} \sqrt{1-E^2} \mathcal{F} \left(\frac{T'^2}{1-E^2} \right) \\ &= \mathcal{T}_1 \int d\tilde{x} e^{-\frac{\tilde{T}^2}{4}} \mathcal{F}(\tilde{T}'^2), \end{aligned} \quad (4.6)$$

which is the same as that for the pure tachyon case. It means that there is a one-to-one correspondence between a kink solution in this $E^2 < 1$ case and that in the pure tachyon case in section 3.1. Indeed, the form of the equation with rescaled variables is the same up to an overall constant

$$-T^{11} = \frac{-\Pi}{E} = \frac{\mathcal{T}_1 V(T)}{\sqrt{1-E^2}} G(y), \quad (4.7)$$

which is rewritten as

$$\mathcal{E}_E = (1 - E^2)K(y) + U(T), \quad (4.8)$$

with $\mathcal{E}_E = -(1 - E^2)$. Note that, in this case, “energy” \mathcal{E}_E depends on the electric field. By varying the value of E , we can obtain different types of solutions.

(i) **Array of kink-antikink:** When magnitude of the electric field is strictly less than the critical value, $E^2 < 1$, the situation is essentially the same as in section 3. That is, when $-T^{11} < \mathcal{T}_1/\sqrt{1-E^2}$, we have array of kink-antikinks as the unique regular static soliton solution of codimension-one, where the tachyon field oscillates between $\pm \tilde{T}_{\max} = \pm 2\sqrt{\ln[\mathcal{T}_1/(-T^{11}\sqrt{1-E^2})]}$.

It is a simple matter to estimate the domain size $\tilde{\xi}$, i.e., the distance between a kink and an adjacent antikink, since the only difference from the previous section is that the spatial coordinate is rescaled by the factor $\sqrt{1-E^2}$. For fixed E , we find that the distance $\tilde{\xi}$ has a maximum $\tilde{\xi}_{\max} = 2\pi\sqrt{2\ln 2}/\sqrt{1-E^2}$ in the vanishing \tilde{T}_{\max} limit ($-T^{11} \rightarrow \mathcal{T}_1/\sqrt{1-E^2}$). As $-T^{11}$ decreases, the size $\tilde{\xi}$ becomes smaller and eventually goes to zero in the infinite \tilde{T}_{\max} limit ($T^{11} \rightarrow 0$). This is the same behavior as in the pure tachyon case.

Note, however, that E can be changed to control the the rescaling factor $\sqrt{1-E^2}$ in the denominator. If the critical limit $E \rightarrow 1$ is taken first for fixed T^{11} , one would find that $\tilde{\xi}$ diverges, which will be discussed shortly. This implies that there exists a sort of limit that both $E \rightarrow 1$ and $T^{11} \rightarrow 0$ are taken simultaneously in such a way that the distance $\tilde{\xi}$ remains finite even when $T^{11} \rightarrow 0$ (or $\Pi \rightarrow 0$ equivalently). A short analysis shows that it happens when the limits are taken keeping

$$(1 - E^2) \ln |T^{11}\sqrt{1-E^2}| = \text{finite}. \quad (4.9)$$

In other words, in this case one can obtain array solutions with arbitrary period even in vanishing T^{11} limit in which the amplitude of tachyon profile becomes infinite. This is somewhat similar to the case of DBI type EFT with $1/\cosh$ potential [10, 17].

From 00-component of the energy-momentum tensor (2.15), we read energy density given by a sum of constant piece and localized piece

$$T_{00} = \frac{\mathcal{T}_1 V(T)}{\sqrt{1-E^2}} G(y)$$

$$= -\Pi E + \mathcal{T}_1 V(T) \sqrt{1 - E^2} \mathcal{F}(y). \quad (4.10)$$

The first constant term stands for the energy density of fundamental string. The second term is localized at the position of (anti)kink and, on integrating over the distance $\tilde{\xi}$, becomes

$$\begin{aligned} \int_{-\tilde{\xi}/2}^{\tilde{\xi}/2} dx \mathcal{T}_1 V(T) \sqrt{1 - E^2} \mathcal{F}(y) &= \int_{-\tilde{\xi}/2}^{\tilde{\xi}/2} d\tilde{x} \mathcal{T}_1 V(T) \mathcal{F}(\tilde{T}'^2) \\ &= 2\pi \mathcal{T}_1 \quad (\text{in large } T_{\max} \text{ limit}). \end{aligned} \quad (4.11)$$

Note that in the first line the factor $\sqrt{1 - E^2}$ is naturally incorporated in \tilde{x} . In the second line we have used the result of the previous section, since it is the same form as (3.9). Therefore we again obtain the decent relation $\mathcal{T}_0 = 2\pi \mathcal{T}_1$, and the obtained array of kink-antikink is identified as array of D0 \bar{D} 0.

(ii) **Topological BPS kink:** When the electric field has critical value $E^2 = 1$, $-\det(\eta + F) = 1 - E^2$ vanishes and y in (4.5) diverges. Physical quantities, however, have well-defined finite limit and actually become quite simplified. To deal with this case properly, we use the following asymptotic form of $\mathcal{F}(y)$ for large y ,

$$\mathcal{F}(y) \approx \sqrt{\pi} y^{\frac{1}{2}} + \frac{\sqrt{\pi}}{8} y^{-\frac{1}{2}} + \mathcal{O}(y^{-\frac{3}{2}}). \quad (4.12)$$

Then, for example, the action in (4.6) becomes

$$\begin{aligned} \frac{S|_{E^2=1}}{-\int dt} &= \lim_{E^2 \rightarrow 1} \mathcal{T}_1 \int_{-\infty}^{\infty} dx e^{-\frac{T^2}{4}} \sqrt{1 - E^2} \left[\frac{\sqrt{\pi} |T'|}{\sqrt{1 - E^2}} + \frac{\sqrt{\pi(1 - E^2)}}{8|T'|} + \mathcal{O}((1 - E^2)^{\frac{3}{2}}) \right] \\ &= \sqrt{\pi} \mathcal{T}_1 \int_{-\infty}^{\infty} dx e^{-\frac{T^2}{4}} |T'| \\ &= \sqrt{2} \pi \sqrt{\alpha'} \mathcal{T}_1 = \mathcal{T}_0. \end{aligned} \quad (4.13)$$

The equations of motion (4.2) and (4.3) reduce to

$$\frac{-\Pi}{E} = -T^{11} = \frac{\sqrt{\pi} \mathcal{T}_1 V}{4|T'|}. \quad (4.14)$$

Solving this equation, we obtain an exact solution satisfying $T'(x = \pm\infty) = 0$ in a closed form,

$$T(x) = \pm 2 \operatorname{erfi}^{-1} \left(\frac{\mathcal{T}_1}{4\Pi} x \right), \quad (4.15)$$

where $\operatorname{erfi}(x)$ is the imaginary error function. The profile of the solution is shown in Fig. 4. Since the solution connects monotonically two vacua at positive and negative

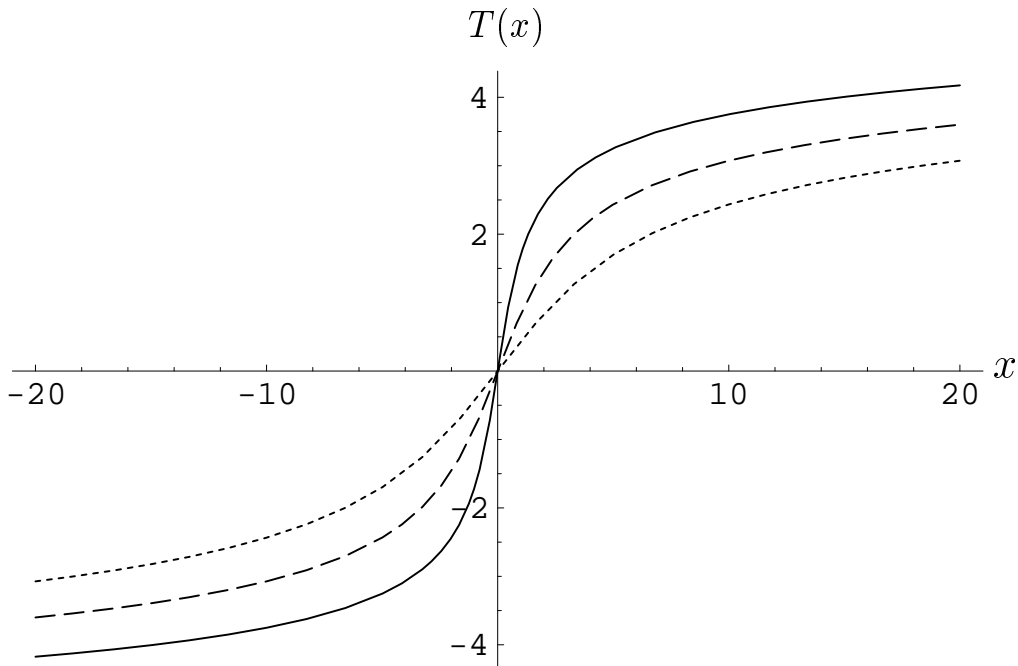


Figure 4: Profiles of single topological BPS kink for the cases $\Pi = -1.0$ (dotted curve), -0.5 (dashed curve), -0.2 (solid curve) as the slopes become steep.

infinity, $T(-\infty) = \mp\infty$ and $T(\infty) = \pm\infty$, the obtained solution is interpreted as single topological tachyon kink (antikink) for the upper (lower) sign.

The corresponding energy density (4.10) is again written as a sum of a constant part and a localized part as shown in Fig. 5,

$$T_{00} = -\Pi + \sqrt{\pi} \mathcal{T}_1 V(T) |T'|. \quad (4.16)$$

The localized part is the same as that appearing in (4.13). As Π goes to zero it becomes sharply peaked near $x = 0$ and approaches $2\pi \mathcal{T}_1 \delta(x)$. The energy is then given by a sum of the D0 charge and the fundamental string charge, Π ,

$$E \equiv \int_{-\infty}^{\infty} dx T_{00} = \mathcal{T}_0 + Q_{F1}, \quad (4.17)$$

which is nothing but a BPS sum rule. Note that this result is obtained regardless of the value of Π which controls the thickness of the kink as seen in the Fig. 5. The solution can be identified as a thick single topological BPS tachyon kink discussed in DBI type EFT [10] and in BCFT [3]. Monotonicity of the tachyon profile for the topological BPS kink (4.15) shown in Fig. 4 may suggest a tip of hint on the field redefinition among the

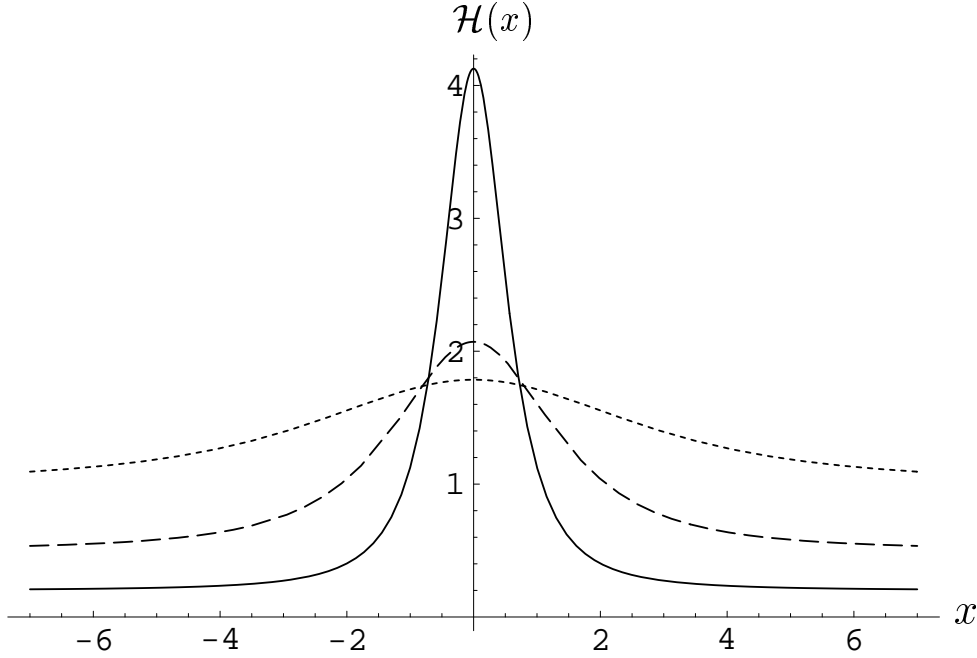


Figure 5: Energy density profiles of single BPS kink for the cases $\Pi = -1.0$ (dotted curve), -0.5 (dashed curve), -0.2 (solid curve) as the slopes become steep. It is clear that their width is decreasing as T_{\max} increases.

tachyon fields in DBI type EFT, BCFT, and BSFT, in which the profiles of topological BPS kink are given by closed functional form. As we shall see, the corresponding energy density profiles are slightly different so that this naive comparison definitely needs further systematic studies.

4.2 Arbitrary $p \geq 2$

The analysis on the unstable D1-brane in the previous section can be easily generalized to unstable Dp -branes with $p \geq 2$. The only difference is that the Bianchi identity, $\partial_\mu F_{\nu\rho} + \partial_\nu F_{\rho\mu} + \partial_\rho F_{\mu\nu} = 0$ is no longer trivial. However, we show shortly that all components of the field strength tensor (4.1) are just constant, and static kink configurations are governed by a single first-order differential equation for the tachyon field, which is similar to the one for the $p = 1$ case. On the other hand, possible solutions are richer than $p = 1$ case; there exist three other types of solutions in addition to the array of kink-antikink and the thick single topological BPS kink in the previous section.

Under the assumption of homogeneous codimension-one objects, the conservation of energy-momentum (2.14) becomes $(T^{1\nu})' = 0$, that is, $T^{1\nu}$ are constant. The expression

for $T^{1\nu}$ simplifies to

$$T^{1\nu} = \frac{\mathcal{T}_p V}{\sqrt{\beta}} C_S^{1\nu} G(y), \quad (4.18)$$

where $\alpha = -C^{11}$ and $\beta = -\det(\eta_{\mu\nu} + F_{\mu\nu})$ with $C_S^{\mu\nu}$ denoting symmetric part of the cofactor of the matrix $(\eta + F)$ and $y = \alpha T'^2/\beta$. The equation for the gauge field (2.12), $(\Pi^{1\nu})' = 0$, also implies constant-valued $\Pi^{1\nu}$ whose expression is

$$\Pi^{1\nu} = \frac{\mathcal{T}_p V}{\sqrt{\beta}} C_A^{1\nu} G(y), \quad (4.19)$$

where $C_A^{1\nu}$ is the anti-symmetric part of the cofactor. From these, we conclude that

$$\frac{\mathcal{T}_p V}{\sqrt{\beta}} C^{1\nu} G(y) = \text{constant}. \quad (4.20)$$

The Bianchi identity imposes $p(p-1)/2$ constraints on the field strength tensor with $p(p+1)/2$ components. With simple checking, it is easy to find that $E^i = -F_{0i}$ and $F_{ij}(i, j \neq 1)$ are constants. In (4.18) with $\nu = 1$, the symmetric part of the cofactor C_S^{11} is constant since it is composed of only E^i and F_{ij} ($i, j \neq 1$). Then (4.18) tells us that

$$\frac{\mathcal{T}_p V}{\sqrt{\beta}} G(y) = \gamma_p = \text{constant}, \quad (4.21)$$

with which (4.20) again implies that $C^{1\nu}$ are constant for all ν 's. When all components of cofactor $C^{1\nu}$ are constant, $F_{1\nu}$'s are also constant as far as the determinant β does not vanish. The case where the determinant vanishes can be treated in a similar fashion as was done in the case of $p = 1$ with $E^2 = 1$. In summary, we have proved that all components of the field strength tensor $F_{\mu\nu}$ are constant, and the only remaining first-order differential equation (4.21) maybe rewritten as

$$\mathcal{E}_p = K_p(y) + U_p(T), \quad (4.22)$$

where

$$\mathcal{E}_p = -\frac{\beta}{2\alpha}, \quad K_p(y) = \frac{\beta}{2\alpha} \left[\frac{1}{(G(y))^2} - 1 \right], \quad U_p = -\frac{\mathcal{T}_p^2 V^2}{2\gamma_p^2 \alpha}. \quad (4.23)$$

This is our primary equation whose solutions we are going to discuss in the following. Physical properties of the solutions are characterized by the following quantities. Charge density of the fundamental strings along the x -direction is a constant of motion,

$$\Pi^1 = \frac{\mathcal{T}_p V}{\sqrt{\beta}} C_A^{01} G(y) = \gamma_p C_A^{01}. \quad (4.24)$$

A new aspect of $p \geq 2$ case is that there are $p - 1$ spatial directions orthogonal to x . The charge densities of the fundamental string along these directions are x -dependent,

$$\Pi^a = \frac{\mathcal{T}_p V}{\sqrt{\beta}} \left[C_A^{0a} \mathcal{F} - 2 \frac{T'^2}{\beta} \dot{\mathcal{F}} (C_A^{10} C_S^{1a} - C_A^{1a} C_S^{10}) \right], \quad (a = 2, 3, \dots, p). \quad (4.25)$$

Using (4.24), these can be written as a sum of a constant part proportional to Π^1 and an x -dependent part as in (4.10),

$$\Pi^a = \frac{1}{\alpha C_A^{01}} (C_A^{10} C_S^{1a} - C_A^{1a} C_S^{10}) \Pi^1 + (\alpha C_A^{0a} - C_A^{10} C_S^{1a} + C_A^{1a} C_S^{10}) \frac{\mathcal{T}_p V}{\alpha \sqrt{\beta}} \mathcal{F}. \quad (4.26)$$

Similarly, the expression for the energy density is given by

$$\begin{aligned} \mathcal{H} = T_{00} &= \frac{\mathcal{T}_p V}{\sqrt{\beta}} \left(C_S^{00} \mathcal{F} + 2 \frac{T'^2}{\beta} \dot{\mathcal{F}} C^{01} C^{10} \right) \\ &= \frac{C^{01} C^{10}}{\alpha C_A^{10}} \Pi^1 + \left(C^{00} + \frac{1}{\alpha} C^{01} C^{10} \right) \frac{\mathcal{T}_p V}{\sqrt{\beta}} \mathcal{F}. \end{aligned} \quad (4.27)$$

Comparing (4.26) and (4.27), we notice that the localized pieces share the same functional shape except for overall coefficients. Therefore, it is enough to look into either the Hamiltonian density (4.27) or the charge density (4.26) when properties of the localized pieces are discussed.

Now we find the solution. Since BSFT action (2.8) is valid only for nonnegative $\beta = -\det(\eta_{\mu\nu} + F_{\mu\nu})$, there are five different cases to consider, depending on the sign of α and the magnitude of β .

(i) **Array of kink-antikink for $\alpha > 0$ and $\beta > 0$** : When both α and β are positive, the mechanical energy \mathcal{E}_p and the potential energy $U_p(T)$ in (4.23) are negative, and our equation (4.22) is identical to the equation (3.6) for the pure tachyon case in the previous section up to a trivial rescaling of the spatial coordinate, $\tilde{x} = \sqrt{(\beta/\alpha)} x$ as done in $p = 1$ case. We then obtain kink-antikink array solutions. The second term of the energy density (4.27) is localized at the sites of kinks and antikinks. Note that the charge densities Π^a in (4.26), which orthogonal to x -direction, also have peak values at (anti)kink sites. This may be interpreted as fundamental strings confined on $D(p-1) \bar{D}(p-1)$ branes.

(ii) **Topological BPS kink for $\alpha > 0$ and $\beta = 0$** : Similarly, $\beta = 0$ corresponds to the critical electric field $E^2 = 1$ in the $p = 1$ case and we obtain a single BPS kink solution in closed form (4.15) with a suitable change of the parameters. Again the only difference is the localization of fundamental strings on the codimension-one D-brane so that the obtained topological BPS kink is $D(p-1)F1$ composite as shown in Fig. 6. We omit the details.

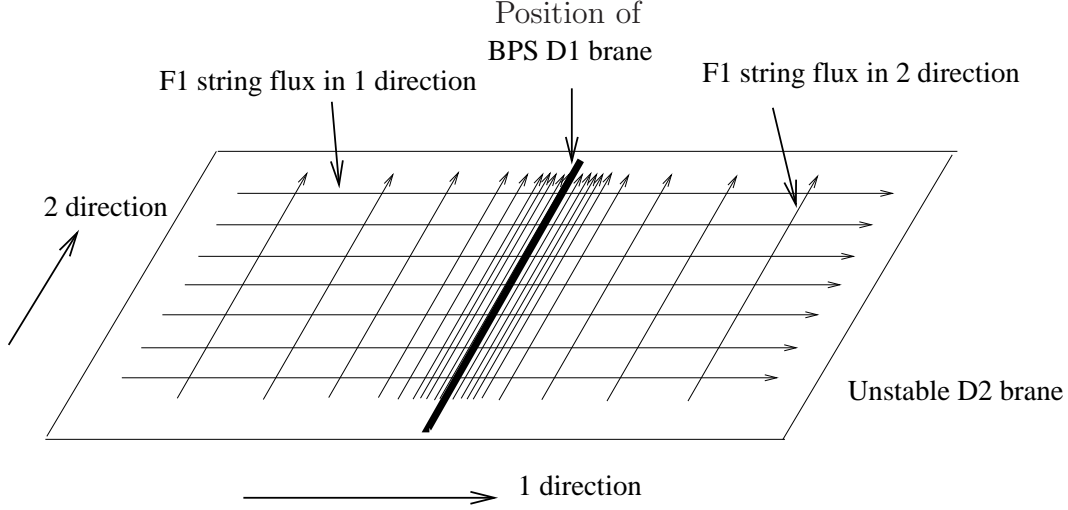


Figure 6: A schematic figure of confined fundamental strings along stable D1-brane from an unstable D2-brane.

Although both the array of kink and antikink and the single topological BPS kink exist on an unstable Dp -brane for any p , the next three cases that we are going to discuss are supported only for $p \geq 2$ and negative α . For these cases, it is convenient to multiply $-\alpha/\beta$ to both sides of our primary equation (4.22), so that the resultant equation coincides formally with that of the homogeneous rolling tachyons [24]

$$\hat{\mathcal{E}}_p = \hat{K}_p(y) + \hat{U}_p(T), \quad (4.28)$$

with,

$$\hat{\mathcal{E}}_p = 1, \quad 1 \geq \hat{K}_p(y) = 1 - \frac{1}{G(y)^2} \geq 0, \quad \hat{U}_p = \frac{\mathcal{T}_p^2 V(T)^2}{\gamma_p^2 \beta} \geq 0, \quad (4.29)$$

for negative $y = \frac{\alpha}{\beta} T'^2$. We draw \hat{K}_p and \hat{U}_p in Fig. 7. We use $\beta \geq 0$ for soliton solutions due to $\max(\hat{K}_p) = 1$ which requires $\hat{\mathcal{E}}_p - \hat{K}_p(y) = \hat{U}_p(T) \geq 0$. Since $\hat{\mathcal{E}}_p$ is fixed to be unity and $d\hat{U}_p/dT$ vanishes only at $T = 0, \pm\infty$, the domain $-1 \leq y \leq 0$ is of our interest for $\hat{K}_p(y)$ which is monotonic decreasing from $\hat{K}_p(-1) = 1$ to $\hat{K}_p(0) = 0$ (see Fig. 7).

When $\beta = 0$, there exist only trivial vacuum solutions at $T = \pm\infty$ and thereby we consider only positive β for nontrivial kinks. $\hat{\mathcal{E}}_p = 1$ provides three situations that the top of \hat{U}_p is higher than $\hat{\mathcal{E}}_p$ (the dotted-dashed line in Fig. 7, $0 < \beta < (\mathcal{T}_p/\gamma_p)^2$), equal to $\hat{\mathcal{E}}_p$ (the solid line in Fig. 7, $\beta < (\mathcal{T}_p/\gamma_p)^2 = 0$), and lower than $\hat{\mathcal{E}}_p$ (the dashed line in Fig. 7, $\beta < (\mathcal{T}_p/\gamma_p)^2 = 0$). We are discussing those three cases below.

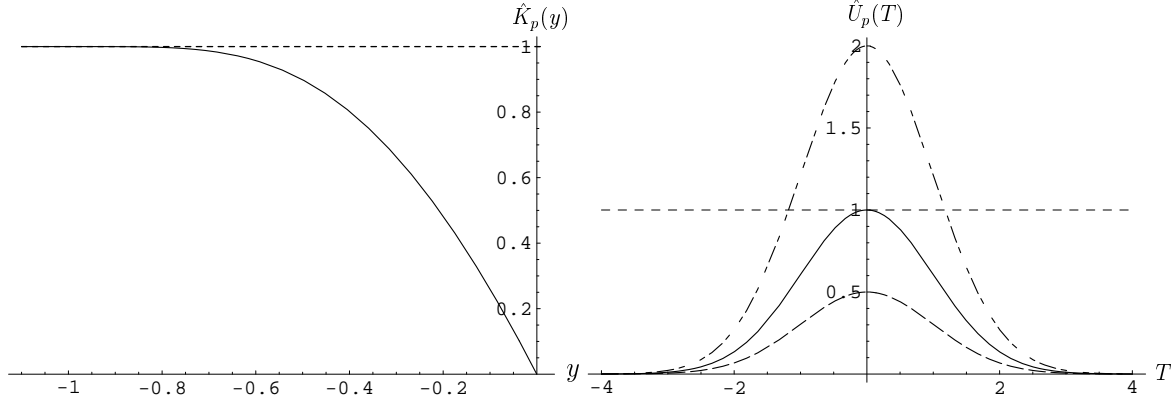


Figure 7: The graphs of $\hat{K}_p(y)$ and $\hat{U}_p(T)$. For $\hat{U}_p(T)$, three cases of $\mathcal{T}_p/(\gamma_p\sqrt{\beta})$ is larger than (dotted-dashed curve, $1/\sqrt{2}$), equal to (solid curve, 1), and smaller than (dashed curve, $\sqrt{2}$) unity from top to bottom are shown. $\hat{\mathcal{E}}_p = 1$ is given by a straight dotted lines in both figures.

(iii) **Bounce for $\alpha < 0$ and $0 < \beta < (\mathcal{T}_p/\gamma_p)^2$:** As shown by the solid line in Fig. 8, we let the bounce solution have its minimum value at $x = 0$; $T(x = 0) = T_{\text{bounce}} = \sqrt{2 \ln \left(\frac{\mathcal{T}_p^2}{\beta \gamma_p^2} \right)}$ with $T'(x = 0) = 0$ (see Fig. 8). Expanding the solution near the turning

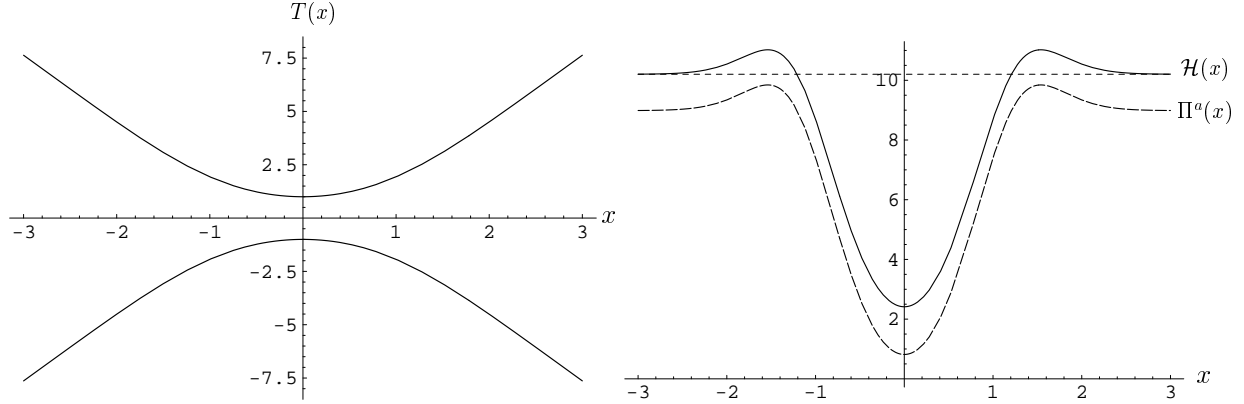


Figure 8: The graphs of bounce for $\mathcal{T}_p^2/(\gamma_p^2\beta) = 1.65 > 1$. The tachyon field $T(x)$ is given in the left figure. The energy density $\mathcal{H}(x)$ (solid line) and the charge density of fundamental strings along the transverse directions Π^a (the dashed line) are given in the right figure.

point, we have

$$T(x) \approx T_{\text{bounce}} + a_b x^2 + \mathcal{O}(x^4), \quad (4.30)$$

where $a_b = \frac{\beta T_{\text{bounce}}}{16 \ln 2 (-\alpha)}$. Inserting this into the energy density (4.27), we get the profile of

the energy density near $x = 0$,

$$\mathcal{H} = T_{00} \approx \frac{\mathcal{T}_p e^{-\frac{T_{\text{bounce}}^2}{4}}}{\sqrt{\beta}} \left\{ C_S^{00} + 16 \ln 2 [C^{01}C^{10} - (-\alpha)C_S^{00}] \frac{a_b^2}{\beta} x^2 + \mathcal{O}(x^4) \right\}. \quad (4.31)$$

In addition to the positive constant leading term, the coefficient of subleading term is also positive which is consistent with numerical result in Fig. 8. To see why this is true, consider an exemplar case of $p = 2$, where we have (we let $x = x^1$)

$$\begin{aligned} \alpha = -C^{11} = 1 - E_2^2 < 0, \quad \beta = -\det(\eta + F) = 1 + B^2 - E_1^2 - E_2^2 > 0, \\ C^{00} = 1 + B^2, \quad C^{01}C^{10} = E_2^2 B^2 - E_1^2, \end{aligned} \quad (4.32)$$

so that

$$C^{01}C^{10} - (-\alpha)C^{00} = \beta > 0. \quad (4.33)$$

Note also that $C^{01}C^{10}$ is always positive.

Near the infinity $x \rightarrow \pm\infty$, using the fact that $G(y)$ blows up at $y \rightarrow -1$ as $G(y) \rightarrow \frac{1}{(y+1)^2} - \frac{3}{2} \frac{1}{(y+1)}$, the tachyon field behaves as (we only focus on the one side where $x \rightarrow \infty$ or $T \rightarrow \infty$ for the other side is symmetric.)

$$T(x) \approx \sqrt{\frac{\beta}{(-\alpha)}} \left[(x - x_0) + \frac{2(-\alpha)\sqrt{\mathcal{T}_p}}{\sqrt{\gamma_p}\beta^{\frac{5}{4}}} \frac{1}{(x - x_0)} e^{-\frac{\beta}{(-8\alpha)}(x-x_0)^2} \right], \quad (4.34)$$

where x_0 is determined only by the boundary condition at $x = -\infty$. Substituting the tachyon profile (4.34) into the energy density (4.27), we obtain the positive constant leading term and the positive but exponentially-decreasing subleading term as

$$\mathcal{H} \approx \frac{\gamma_p}{(-\alpha)} C^{01}C^{10} + \frac{\sqrt{\gamma_p\mathcal{T}_p}}{2(-\alpha)\beta^{\frac{1}{4}}} [C^{01}C^{10} - (-\alpha)C^{00}] e^{-\frac{\beta}{8(-\alpha)}(x-x_0)^2}. \quad (4.35)$$

The obtained asymptotic profile (4.35) is consistent with numerical result in Fig. 8.

In the above, if we subtract the asymptotic constant piece, which is due to condensation of the fundamental strings on the Dp -brane represented by the constant electromagnetic field strength, we can interpret the resulting energy profile as the bound energy of a composite of the tachyon bounce and confined fundamental strings. By studying numeric solutions, Fig. 8, it is interesting to note that the energy and Π^a profiles (after subtracting their asymptotic values at infinity) have a positive bump at some finite distance from the center. We see that there exists a position x_* such that $\mathcal{H}(x_*) = \mathcal{H}(\pm\infty)$ and $\Pi^a(x_*) = \Pi^a(\infty)$, although it is not possible to express it analytically. From the Fig. 8, we read that a localized bounce with negative energy is formed by repelling the condensed DBI

electromagnetic field. Therefore, this composite may be interpreted as a negative energy *brane* of codimension-one, generated through *de-condensing* the background fundamental strings with positive constant energy density.

Note that the obtained asymptotic behavior (4.34) can also be applied to other soliton solutions with $\beta > 0$ and $\alpha < 0$ given below. However they are different from those from DBI type EFT [10, 17]. Since the profiles of energy-momentum tensors in BCFT and DBI type EFT are qualitatively the same, we expect that if these soliton configurations are reproduced in the context of BCFT, their asymptotic behaviors would probably be slightly different from what we achieved here in BSFT.

(iv) **Half-kink for $\alpha < 0$ and $\beta = (\mathcal{T}_p/\gamma_p)^2$:** When $\beta = (\mathcal{T}_p/\gamma_p)^2$, we have a half-kink solution satisfying $T(x = -\infty) = 0$ and $T(x = \infty) = \pm\infty$ (see Fig. 9). The leading

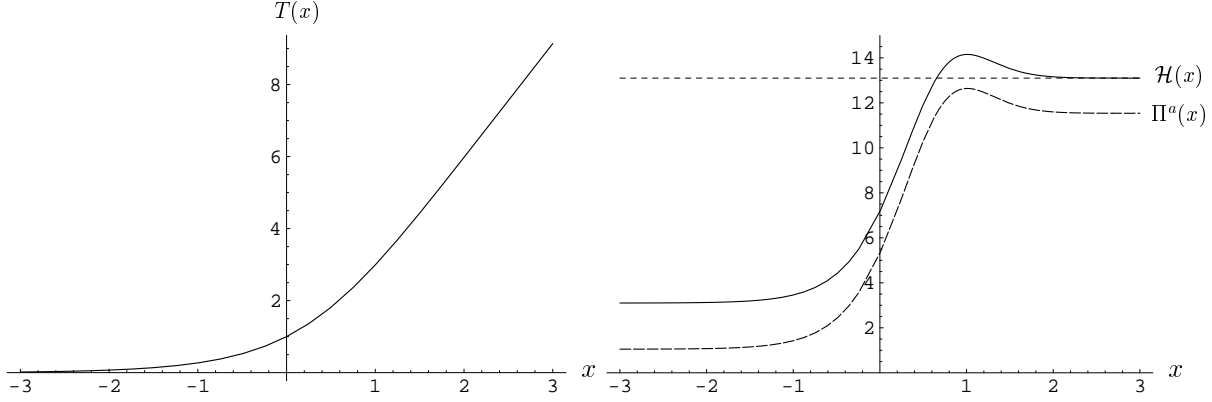


Figure 9: The graphs of half kink for $\mathcal{T}_p^2/(\gamma_p^2\beta) = 1$. The tachyon field $T(x)$ is given in the left figure. The energy density $\mathcal{H}(x)$ (solid line) and the charge density of fundamental strings along the transverse directions Π^a (dashed line) are given in the right figure.

behavior of the tachyon around $x = -\infty$ is exponential as expected,

$$T(x) \approx e^{a_h x} + \dots, \quad (4.36)$$

and then behavior of the physical quantity (4.25) (or (4.27)) around $x = -\infty$ is easily shown to be

$$\mathcal{H} \approx \frac{\mathcal{T}_p}{\sqrt{\beta}} \left[C_s^{00} + \frac{1}{2(-\alpha)} (C^{01}C^{10} - (-\alpha)C_s^{00}) e^{2a_h x} \right] + \dots, \quad (4.37)$$

where $a_h = \sqrt{\frac{\beta}{8 \ln 2(-\alpha)}}$. In (4.37), the leading term is constant and the coefficient of the subleading term for the energy density is positive as before. In the exemplar case of $p = 2$,

we have by (4.33), (note that $\frac{\mathcal{T}_p}{\sqrt{\beta}} = \gamma_p$ in our case)

$$\mathcal{H}(-\infty) = \left(\frac{\mathcal{T}_p}{\sqrt{\beta}} \right) C_S^{00} = \gamma_p C_S^{00} < \frac{\gamma_p}{(-\alpha)} C^{01} C^{10} = \mathcal{H}(\infty), \quad (4.38)$$

and we again find that there is a point x_* such that $\mathcal{H}(x_*) = \mathcal{H}(\infty)$ and $\Pi^a(x_*) = \Pi^a(\infty)$. Also, $C_A^{02} = -E_2$, and $C_A^{10} C_S^{12} - C_A^{12} C_S^{10} = E_2(E_1^2 + B^2)$, so that we have

$$\Pi^2(-\infty) = \left(\frac{\mathcal{T}_p}{\sqrt{\beta}} \right) C_A^{02} = \gamma_p(-E_2), \quad \Pi^2(\infty) = \frac{\gamma_p}{(-\alpha)}(-E_2)(E_1^2 + B^2), \quad (4.39)$$

and they have the same direction.

The half kink configuration connects smoothly the false symmetric vacuum at $T = 0$ and the true broken vacua at $T = \pm\infty$ so that this static object forms a boundary of two phases. Therefore, it can be interpreted as a *half brane* ($\frac{1}{2}\text{D}(p-1)$ -brane) similar to bubble wall at a given time. The profile of $\Pi^a(x)$ in Fig. 9 suggests that the fundamental strings that are condensed in the true and the false vacuum align in the same direction. In the case of DBI type EFT and NCFT, after subtracting the vacuum energy from the unstable vacuum, the total energy of the half kink solution vanishes exactly [19]. Though we need careful analysis to answer this in BSFT, it is at least the configuration of almost zero energy. Usually a bubble wall produced with radius larger than critical value starts to expand by consuming vacuum energy of the false vacuum. Therefore, it may be intriguing to ask such dynamical questions for this half brane.

(v) **Topological nonBPS kink for $\alpha < 0$ and $\beta > (\mathcal{T}_p/\gamma_p)^2$:** This case describes topological nonBPS kinks connecting both vacua $T \rightarrow \pm\infty$ as shown in Fig. 10.

If we restrict our analysis to cases where β is very close to $(\mathcal{T}_p/\gamma_p)^2$ so that $T'(x=0) \ll 1$ when the tachyon is near the top of the tachyon potential at $x = 0$, we can approximate $\frac{1}{G(y)} \sim 1 + (2 \ln 2)y$ for $y \ll 1$, and

$$T(x) \approx a_t x + \frac{1}{3} b_t x^3 + \mathcal{O}(x^5), \quad (4.40)$$

where

$$\begin{aligned} a_t &= \sqrt{\frac{\beta}{2 \ln 2 (-\alpha)} \left(1 - \frac{\mathcal{T}_p}{\sqrt{\beta} \gamma_p} \right)}, \\ b_t &= a_t \frac{\mathcal{T}_p \sqrt{\beta}}{(16 \ln 2) (-\alpha) \gamma}. \end{aligned} \quad (4.41)$$

Substituting this into the energy density (4.27), we obtain near $x = 0$,

$$\mathcal{H} \approx \frac{\mathcal{T}_p}{\sqrt{\beta}} \left[C_S^{00} \left(\frac{\mathcal{T}_p}{\sqrt{\beta} \gamma_p} \right) + \frac{2}{(-\alpha)} \left(1 - \frac{\mathcal{T}_p}{\sqrt{\beta} \gamma_p} \right) C^{01} C^{10} \right] \quad (4.42)$$

$$- \frac{\mathcal{T}_p}{\sqrt{\beta}} \frac{\beta}{(4 \ln 2) (-\alpha)} \left(1 - \frac{\mathcal{T}_p}{\sqrt{\beta} \gamma_p} \right) \left[C_S^{00} \frac{\mathcal{T}_p}{\sqrt{\beta} \gamma_p} + \frac{C^{01} C^{10}}{(-\alpha)} \left(1 - \frac{2\mathcal{T}_p}{\sqrt{\beta} \gamma_p} \right) \right] x^2. \quad (4.43)$$

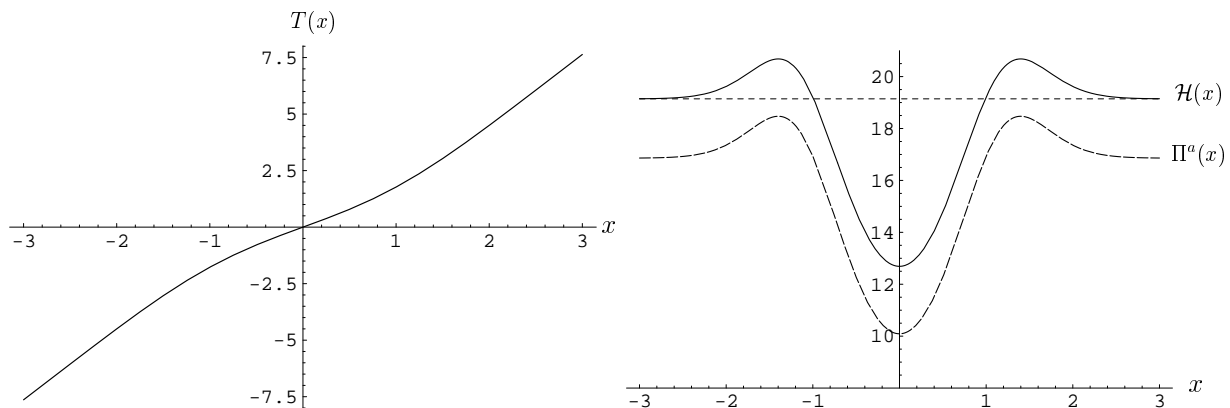


Figure 10: The graphs of nonBPS topological kink for $\mathcal{T}_p^2/(\gamma_p^2\beta) = 0.47 < 1$. The tachyon field $T(x)$ is given in the left figure. The energy density $\mathcal{H}(x)$ (solid line) and the charge density of fundamental strings along the transverse directions Π^a (dashed line) are given in the right figure.

Similar to the previous solutions, the leading term in (4.43) is constant and the coefficient of the second term is positive. Though the profile of the tachyon is different from that of the bounce in Fig. 8, the energy density and the string charge density of the nonBPS topological kink resemble those of the bounce. Therefore, the same arguments in the case of bounce can be repeated and we omit those. Due to their boundary conditions, the bounce may be an unstable object but the nonBPS topological kink is a stable soliton. At any rate the obtained nonBPS topological kink can be interpreted as a *brane* with finite negative tension where the condensed fundamental strings are repelled.

There have been found similar nonBPS topological kink solutions in DBI type EFT for both $\alpha > 0$ and $\beta < 0$. Since the tachyon action of our interest (2.8) is not valid in the range of $\beta < 0$, we only find the solutions for $\beta > 0$.

5 Conclusion and Outlook

We studied effective theory of a real tachyon and abelian gauge field in the framework of BSFT, describing a system of an unstable Dp -brane with fundamental strings in superstring theory. Static kink configurations and their interpretation as codimension-one branes were of our interest.

When gauge field is absent, there exists a unique solution of the array of kink-antikink and it is identified as an array of $D(p-1)\bar{D}(p-1)$. This uniqueness coincides with the

results of BCFT [3] and DBI type EFT [7, 10]. In the presence of the gauge field, we found rich spectrum of static solitons including array of kink-antikink, topological BPS kink, bounce, half-kink, and nonBPS topological kink. It is also consistent with the result of DBI type EFT [10, 17] and NCFT [19]. For the topological BPS kink, we find a closed functional form of the tachyon field profile. Since we also have exact solution of this BPS kink in DBI type EFT [10] and BCFT [3], we may read a tip of field redefinition between the tachyon field in BSFT and that in BCFT.

In the context of superstring theory, interpretation of some of the above objects is clear. To be specific, the array of kink-antikink should be an array of $D(p-1)\bar{D}(p-1)$ or that of $D(p-1)F1\bar{D}(p-1)F1$ where some fundamental strings are confined on D-brane. The topological BPS kink is a single BPS $D(p-1)$ -brane or $D(p-1)F1$ composite out of unstable Dp -brane. Our analysis also suggests an interpretation for other three solitonic configurations. The bounce connecting the same unstable vacuum may be an unstable brane of negative tension formed by repelling the condensed background fundamental strings. The nonBPS topological kink may be a stable brane of negative tension by decondensing fundamental strings on it. The half-kink must be an intriguing object, which connects the false symmetric vacuum and the true broken vacuum so that it seems like a static domain wall forming a boundary of two phases. It is a half-brane describing $(p-1)$ -dimensional boundary of the unstable Dp -brane in the middle of decay.

Array of kink-antikink and topological BPS kink have been obtained in BCFT [3], while the latter three configurations have not been found in BCFT, yet. According to BSFT, EFT, and NCFT, the latter three brane configurations are likely to exist in BCFT too, so that they can be established as brane configurations in superstring theory. The present BSFT analysis opens a possibility of study including off-shell contributions.

Acknowledgements

This work was supported by the Science Research Center Program of the Korea Science and Engineering Foundation through the Center for Quantum Spacetime(CQeST) of Sogang University with grant number R11-2005-021(C.K.), and is the result of research activities (Astrophysical Research Center for the Structure and Evolution of the Cosmos (ARCSEC)) supported by Korea Science & Engineering Foundation(Y.K. and O.K.). H.U.Y. is supported by grant No. R01-2003-000-10391-0 from the Basic Research Program of the Korea Science & Engineering Foundation.

A Pressureless Limit of Array Solution

Here we give a detailed analysis on the distance between kink and adjacent antikink in the pressureless limit $T^{11} \rightarrow 0$ ($T_{\max} \rightarrow \infty$) for pure tachyon case of section 3.

In terms of the function $G(y)$ in (3.3), the expression of pressure (3.2) is written as

$$\frac{-T^{11}}{\mathcal{T}_p} e^{\frac{1}{4}T^2} = e^{\frac{1}{4}(T^2 - T_{\max}^2)} = G(y). \quad (\text{A.1})$$

We are interested in the cases of deep potential well where $0 < -T^{11} \ll \mathcal{T}_p$, so that the left-hand side of (A.1) is much less than unity unless $T \sim T_{\max} = \sqrt{\ln|\mathcal{T}_p/T^{11}|} \gg 1$. Let us focus on the kink case, $T' > 0$, in detail because an anti-kink profile is a simple flipped copy of that of a kink. Qualitatively speaking, when $T \ll T_{\max}$, (A.1) tells us $G(T'^2) \ll 1$ which implies that $T' \gg 1$ and the tachyon grows very fast. As T approaches T_{\max} , the left-hand side of (A.1) goes to unity and we have $T' \rightarrow 0$ as $G(T'^2) \rightarrow 1$. Tachyon profile turns around at the point $T = T_{\max}$.

More precisely, $G(T'^2) \ll 1$ when $T \leq T_{\max} - \frac{2}{T_{\max}} \log(T_{\max})$, so that $e^{\frac{1}{4}(T^2 - T_{\max}^2)} \leq \frac{1}{T_{\max}} \ll 1$. We call this kink region. On the other hand, when $(T_{\max} - T)T_{\max} \ll 1$, we would have $G(T'^2) \sim 1$, and for a consistent analysis, we define the plateau region to be $T \geq T_{\max} - \frac{2}{T_{\max} \log(T_{\max})}$. The transition region will then be $T_{\max} - \frac{2}{T_{\max}} \log(T_{\max}) \leq T \leq T_{\max} - \frac{2}{T_{\max} \log(T_{\max})}$. We therefore analyze (A.1) in three separate regions and we interpolate these regions. We will show that the width of each region vanishes as T_{\max} goes to infinity.

In the kink region, we can approximate $G(T'^2) \approx \frac{\sqrt{\pi}}{4} \frac{1}{T'} \ll 1$, because $T' \gg 1$ as we have seen in the above. Using this, (A.1) is integrated at once to give us

$$\int_0^{T(x)} e^{\frac{1}{4}t^2} dt = \frac{\sqrt{\pi}}{4} \left(\frac{\mathcal{T}_p}{-T^{11}} \right) x = \frac{\sqrt{\pi}}{4} e^{\frac{1}{4}T_{\max}^2} x. \quad (\text{A.2})$$

For small $T(x)$, we have

$$T(x) \approx \frac{\sqrt{\pi}}{4} e^{\frac{1}{4}T_{\max}^2} x + \mathcal{O}(x^3), \quad (\text{A.3})$$

and this solution is valid until $T \sim \mathcal{O}(T_{\max}) \gg 1$. In addition, using

$$\int_0^T e^{\frac{1}{4}t^2} dt \approx \frac{2}{T} e^{\frac{1}{4}T^2}, \quad (\text{A.4})$$

for large $T \gg 1$, we have

$$x \sim \frac{8}{\sqrt{\pi}T} e^{\frac{1}{4}(T^2 - T_{\max}^2)}, \quad (\text{A.5})$$

for $T \sim \mathcal{O}(T_{\max})$. Therefore, we see that the kink region has a width of $\Delta x \sim \frac{8}{\sqrt{\pi}} \left(\frac{1}{T_{\max}} \right)^2 \ll 1$. In other words, the tachyon profile grows very fast up to $\mathcal{O}(T_{\max})$ in a narrow region of $\mathcal{O}(1/T_{\max}^2)$.

We next analyze the plateau region where T is much close to T_{\max} . Since the left-hand side of (A.1) is $\mathcal{O}(1)$, we have $T' \sim 0$ as $G(T'^2) \rightarrow 1$ so that we can approximate $G(T'^2) \approx 1 - (2 \log 2) T'^2$. Defining $\Delta T \equiv T - T_{\max}$ and linearizing (A.1) with respect to ΔT , we get

$$\Delta T' \approx \sqrt{\left(\frac{T_{\max}}{4 \log 2} \right)} (-\Delta T), \quad (\text{A.6})$$

which is integrated to be

$$\Delta T \approx - \left(\frac{T_{\max}}{16 \log 2} \right) (x - x_0)^2, \quad (\text{A.7})$$

where x_0 is the turning point of the tachyon profile. The width of this region is easily calculated by letting $\Delta T = -\frac{2}{T_{\max} \log(T_{\max})} \frac{1}{T_{\max}}$ to get $\Delta x = \sqrt{\frac{32 \log 2}{\log(T_{\max})}} \frac{1}{T_{\max}}$, which becomes zero as $T_{\max} \rightarrow \infty$. Note that the gradient of tachyon profile in (A.7) is very steep as $T_{\max} \rightarrow \infty$ and this profile crosses over to a even steeper profile (A.2) of the kink region.

The analysis of the transition region turns out to be much more subtle, especially the width of the region. Defining $u \equiv T_{\max}(T_{\max} - T)$, the equation (A.1) approximates well to

$$G(u'^2/T_{\max}^2) = e^{-\frac{u}{2}}. \quad (\text{A.8})$$

Through a tedious but straightforward analysis of the above equation, we find that the width Δx is of order $\mathcal{O}(1/T_{\max})$, so that this dominates over those of the other two regions. This establishes that the whole width of a single kink becomes zero as $T_{\max} \rightarrow \infty$.

Now let us estimate the energy. Looking at the energy density (3.9), and $\mathcal{F}(x) \approx \sqrt{\pi x} + \mathcal{O}(x^{-\frac{1}{2}})$ for $x \gg 1$, we see that the energy density in the kink region is

$$T^{00} \approx \sqrt{\pi} \mathcal{T}_p e^{-\frac{1}{4} T^2} |T'| \approx \frac{\pi}{4} \mathcal{T}_p e^{-\frac{1}{2} T^2 + \frac{1}{4} T_{\max}^2}, \quad (\text{A.9})$$

which is highly peaked near $T = 0$. Moreover, the solution (A.7) around $T \sim T_{\max}$ shows that $|T'| \gg 1$ unless $(x - x_0) \sim \mathcal{O}(1/T_{\max})$, which in turn corresponds to $\Delta T \sim \mathcal{O}(1/T_{\max})$. This means that the validity of the approximation $\mathcal{F}(T'^2) \approx \sqrt{\pi} T'$ we have used before extends up to $T = T_{\max} - \mathcal{O}(1/T_{\max})$. Therefore, the energy integral for a kink approximates to

$$\int T^{00} dx \sim \sqrt{\pi} \mathcal{T}_p \int e^{-\frac{1}{4} T^2} T' dx = \sqrt{\pi} \mathcal{T}_p \int e^{-\frac{1}{4} T^2} dT, \quad (\text{A.10})$$

with the integration region $-T_{\max} + \mathcal{O}(1/T_{\max}) \leq T \leq T_{\max} - \mathcal{O}(1/T_{\max})$. Using $\mathcal{F}(x) \approx 1 + \mathcal{O}(x)$ for $x \ll 1$, the contribution from the region $\Delta T \leq \mathcal{O}(1/T_{\max})$ can be shown to be of order $\mathcal{O}\left(\frac{\mathcal{T}_p}{T_{\max}} e^{-\frac{1}{4}T_{\max}^2}\right)$, which is negligible. Hence, the topological nature of a kink(anti-kink) energy becomes extremely good as $T_{\max} \rightarrow \infty$ ($T^{11} \rightarrow 0$), and its value goes to

$$\mathcal{T}_{p-1} = \sqrt{\pi} \mathcal{T}_p \int_{-\infty}^{\infty} e^{-\frac{1}{4}T^2} dT = 2\pi \mathcal{T}_p = (2\pi\sqrt{\alpha'}) \frac{\mathcal{T}_p}{\sqrt{2}}. \quad (\text{A.11})$$

This establishes (3.12).

B Comparison with Bosonic Boundary String Field Theory

In this appendix we look into possible tachyon kink solutions in bosonic BSFT [4]. Differently from the super BSFT, the tachyon potential is exact but its kinetic term is approximate because of impossibility of exact computation of the worldsheet beta function. When higher-derivative terms are neglected, the tachyon action is given as

$$S_B = -\mathcal{T}_p \int d^{p+1}x \left[2e^{-T} \partial_\mu T \partial^\mu T + (T+1)e^{-T} + \dots \right], \quad (\text{A.12})$$

where the exact tachyon potential involves instability of the bosonic string theory for negative T and that of the unstable Dp -brane for positive T as shown in Fig. 11 (left).

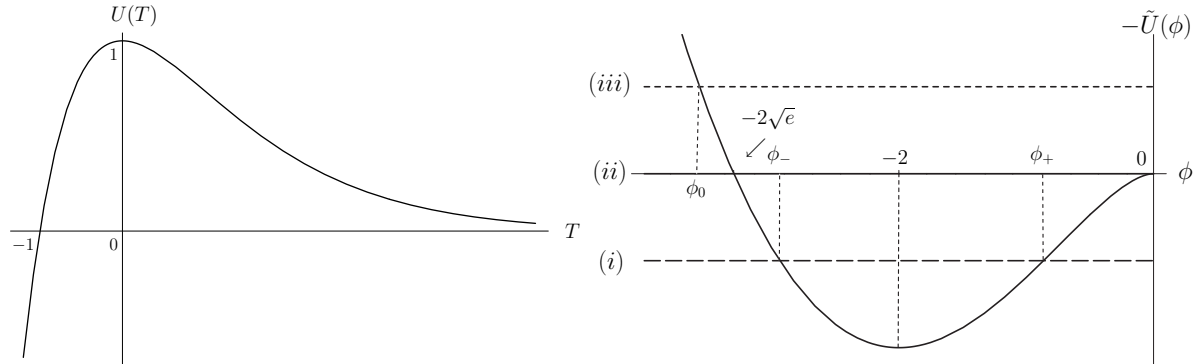


Figure 11: The graphs of $K(x^2)$ (left) and $U(x)$ (right). For $U(x)$, three cases of $\left(\frac{\mathcal{T}_p}{-T^{11}}\right) = \frac{1}{\sqrt{2}}, 1, \sqrt{2}$ from top to bottom are shown.

A field redefinition of the tachyon $\phi = -2e^{-\frac{T}{2}}$ lets the quadratic derivative term have a canonical form,

$$S_B = -\mathcal{T}_p \int d^{p+1}x \left[2\partial_\mu \phi \partial^\mu \phi + \tilde{U}(\phi) \right], \quad (\text{A.13})$$

and then the shape of tachyon potential as a function of the redefined tachyon field ϕ ,

$$\tilde{U}(\phi) = \left[1 - \ln \left(\frac{\phi}{2} \right)^2 \right] \left(\frac{\phi}{2} \right)^2, \quad (\text{A.14})$$

resembles that from vacuum string field theory [REF], i.e., the distance between the local maximum at $\phi = -2$ and the local minimum at $\phi = 0$ is finite.

Under the static ansatz of the tachyon kink $\phi = \phi(x)$, the following first-order equation is obtained

$$\tilde{\mathcal{E}} = \dot{\phi}^2 + \frac{-\tilde{U}}{2}. \quad (\text{A.15})$$

According to value of the integration constant $\tilde{\mathcal{E}}$, analysis can be made by dividing the cases into three (see the dashed line of (i), the solid line of (ii), and the dotted line (iii) in Fig. 11 (right)). When $\tilde{\mathcal{E}} > 0$ (see (iii)), absence of the potential for positive ϕ does not allow a proper kink configuration which spans whole range of x . Array of kink and antikink for $-1 < \tilde{\mathcal{E}} < 0$ (see (i)) is likely to be a natural solution consistent with that in the super BSFT in section 3. For the critical value $\tilde{\mathcal{E}} = 0$, there seems to exist a pair of kink and antikink, but its existence should be confirmed by further study including all the higher derivative terms.

References

- [1] For a review, see A. Sen, “Tachyon dynamics in open string theory,” *Int. J. Mod. Phys. A* **20**, 5513 (2005) [arXiv:hep-th/0410103], and references therein.
- [2] A. Sen, “Rolling tachyon,” *JHEP* **0204**, 048 (2002) [arXiv:hep-th/0203211].
- [3] A. Sen, “Open and closed strings from unstable D-branes,” *Phys. Rev. D* **68**, 106003 (2003) [arXiv:hep-th/0305011].
- [4] A. A. Gerasimov and S. L. Shatashvili, “On exact tachyon potential in open string field theory,” *JHEP* **0010**, 034 (2000) [arXiv:hep-th/0009103];
D. Kutasov, M. Marino and G. W. Moore, “Some exact results on tachyon condensation in string field theory,” *JHEP* **0010**, 045 (2000) [arXiv:hep-th/0009148].
- [5] D. Kutasov, M. Marino and G. W. Moore, “Remarks on tachyon condensation in superstring field theory,” arXiv:hep-th/0010108.
- [6] S. Sugimoto and S. Terashima, “Tachyon matter in boundary string field theory,” *JHEP* **0207**, 025 (2002) [arXiv:hep-th/0205085];

- [7] N. Lambert, H. Liu and J. Maldacena, “Closed strings from decaying D-branes,” arXiv:hep-th/0303139.
- [8] J. A. Minahan and B. Zwiebach, “Effective tachyon dynamics in superstring theory,” JHEP **0103**, 038 (2001) [arXiv:hep-th/0009246].
- [9] A. Sen, “Dirac-Born-Infeld action on the tachyon kink and vortex,” Phys. Rev. D **68**, 066008 (2003) [arXiv:hep-th/0303057].
- [10] C. Kim, Y. Kim and C. O. Lee, “Tachyon kinks,” JHEP **0305**, 020 (2003) [arXiv:hep-th/0304180].
- [11] R. Gopakumar, S. Minwalla and A. Strominger, “Noncommutative solitons,” JHEP **0005**, 020 (2000) [arXiv:hep-th/0003160];
K. Dasgupta, S. Mukhi and G. Rajesh, “Noncommutative tachyons,” JHEP **0006**, 022 (2000) [arXiv:hep-th/0005006];
J. A. Harvey, P. Kraus, F. Larsen and E. J. Martinec, “D-branes and strings as non-commutative solitons,” JHEP **0007**, 042 (2000) [arXiv:hep-th/0005031].
- [12] P. Kraus and F. Larsen, “Boundary string field theory of the DD-bar system,” Phys. Rev. D **63**, 106004 (2001) [arXiv:hep-th/0012198];
T. Takayanagi, S. Terashima and T. Uesugi, “Brane-antibrane action from boundary string field theory,” JHEP **0103**, 019 (2001) [arXiv:hep-th/0012210].
- [13] P. Brax, J. Mourad and D. A. Steer, “Tachyon kinks on non BPS D-branes,” Phys. Lett. B **575**, 115 (2003) [arXiv:hep-th/0304197].
- [14] E. J. Copeland, P. M. Saffin and D. A. Steer, “Singular tachyon kinks from regular profiles,” Phys. Rev. D **68**, 065013 (2003) [arXiv:hep-th/0306294].
- [15] C. Kim, Y. Kim, O. K. Kwon and P. Yi, “Tachyon tube and supertube,” JHEP **0309**, 042 (2003) [arXiv:hep-th/0307184];
W. H. Huang, “Tachyon tube on non BPS D-branes,” JHEP **0408**, 060 (2004) [arXiv:hep-th/0407081].
- [16] Y. Kim, B. Kyae and J. Lee, “Global and local D-vortices,” JHEP **0510**, 002 (2005) [arXiv:hep-th/0508027];
I. Cho, Y. Kim and B. Kyae, “DF-strings from D3 D3-bar as cosmic strings,” arXiv:hep-th/0510218.

- [17] C. Kim, Y. Kim, O-K. Kwon and C. O. Lee, “Tachyon kinks on unstable Dp-branes,” JHEP **0311**, 034 (2003) [arXiv:hep-th/0305092].
- [18] D. Kutasov and V. Niarchos, “Tachyon effective actions in open string theory,” Nucl. Phys. B **666**, 56 (2003) [arXiv:hep-th/0304045].
- [19] R. Banerjee, Y. Kim and O K. Kwon, “Noncommutative tachyon kinks as D(p-1)-branes from unstable D p-brane,” JHEP **0501**, 023 (2005) [arXiv:hep-th/0407229];
Y. Kim, O K. Kwon and C. O. Lee, “Domain walls in noncommutative field theories,” JHEP **0501**, 032 (2005) [arXiv:hep-th/0411164].
- [20] C. Kim, Y. Kim, O-K. Kwon, and H.-U. Yee, in preparation.
- [21] E. Witten, “On background independent open string field theory,” Phys. Rev. D **46**, 5467 (1992) [arXiv:hep-th/9208027]; “Some computations in background independent off-shell string theory,” Phys. Rev. D **47**, 3405 (1993) [arXiv:hep-th/9210065];
S. L. Shatashvili, “Comment on the background independent open string theory,” Phys. Lett. B **311**, 83 (1993) [arXiv:hep-th/9303143], “On the problems with background independence in string theory,” Alg. Anal. **6**, 215 (1994) [arXiv:hep-th/9311177];
K. Li and E. Witten, “Role of short distance behavior in off-shell open string field theory,” Phys. Rev. D **48**, 853 (1993) [arXiv:hep-th/9303067].
- [22] M. Marino, “On the BV formulation of boundary superstring field theory,” JHEP **0106**, 059 (2001) [arXiv:hep-th/0103089];
V. Niarchos and N. Prezas, “Boundary superstring field theory,” Nucl. Phys. B **619**, 51 (2001) [arXiv:hep-th/0103102].
- [23] A. A. Tseytlin, “Renormalization Of Mobius Infinities And Partition Function Representation For String Theory Effective Action,” Phys. Lett. B **202**, 81 (1988);
O. D. Andreev and A. A. Tseytlin, “Partition Function Representation For The Open Superstring Effective Action: Cancellation Of Mobius Infinities And Derivative Corrections To Born-Infeld Lagrangian,” Nucl. Phys. B **311**, 205 (1988).
- [24] A. Ishida, Y. Kim, and S. Kouwn, “Homogeneous Rolling Tachyons in Boundary String Field Theory,” hep-th/0601nnn.